A Precise Measurement of the Nuclear Dependence of Structure Functions in Light Nuclei.

J. Arrington (spokesperson), F. Dohrmann, D. F. Geesaman, H. E. Jackson, B. Mueller, T. G. O'Neill, D. H. Potterveld, P. E. Reimer, B. Zeidman
Argonne National Laboratory, Argonne, IL

P. Gueye, C. E. Keppel, I. Niculescu
Hampton University, Hampton, VA

R. Ent, A. F. Lung, D. J. Mack
Jefferson Laboratory, Newport News, VA

D. Gaskell
Oregon State University, Corvallis, OR

H. Mkrtchyan
Yerevan Physics Institute, Armenia

May 31, 2000

Abstract

We propose to measure inclusive electron scattering from light nuclei over a broad range of x ($0.3 < x < 1.0$) up to $Q^2 \approx 8.0(\mathrm{GeV/c})^2$. We will take data on hydrogen, deuterium, ^{3}He, and ^{4}He to make a precision measurement of the EMC effect (ratio of nuclear to deuteron cross section). The EMC effect has been measured on ^{4}He, but the uncertainty is large enough that it cannot distinguish between different models for the A-dependence in light nuclei. We will improve on existing ^{4}He measurements, as well as making the first measurement of the EMC effect on ^{3}He for $x > 0.5$. This will have a significant impact on our understanding of the A-dependence of the EMC effect for light nuclei, allowing us to test models of the EMC effect and providing guidance for calculations that try to model nuclear effects in deuterium. We will also extract the neutron structure function by comparing the deuteron and proton cross sections. Additionally, the ^{3}He and ^{4}He measurements will test models of nuclear effects which are used to extract the neutron structure function. This will also allow for a better understanding of the systematic uncertainties in the procedure used to extract the neutron structure function from measurements on nuclear targets.

1 INTRODUCTION

Lepton scattering is one of the best ways to gain information on the quark substructure of nucleons and nuclei. The interaction of the electromagnetic probe with the quarks is well understood theoretically, and the relatively weak coupling allows for a clean separation of the scattering mechanism from the target structure. The weak coupling is especially important in probing nuclei, because the scattering is not strongly modified by additional interactions with the target. Leptonic probes have been used to make precise measurements of the polarized and unpolarized structure functions of the proton. The parton model predicts that at large momentum transfer, q, and energy transfer, ν, the structure functions depend only on Bjorken-x [$x = (q^2 - \nu^2)/2m_p\nu = Q^2/2m_p\nu$]. The structure functions measured in this limit can be directly related to the quark distributions within the nucleon, allowing one to extract polarized and unpolarized quark distributions within the proton. The same holds true for lepton scattering from nuclear targets. The structure function in the scaling limit can be related to the quark distributions in the nucleus. This not only provides information on the quark structure of nuclei, but is also our best method of obtaining information on the neutron structure function. Direct scattering measurements from neutrons are not feasible since neutron targets of adequate density are not available. Therefore, most of the information on (unpolarized) neutron structure comes from comparisons of the proton and deuteron structure functions. Extraction of the neutron structure function depends not only on precise measurements on the proton and deuteron, but also on the understanding of nuclear effects in the deuteron. The European Muon Collaboration (EMC) discovered [1] that the nuclear structure function is significantly different from the proton structure function, showing that these nuclear effects are non-trivial. Measurements of the EMC effect in light nuclei will provide guidance for modeling of nuclear effects in the deuteron, which must be understood to extract the neutron structure function. These measurements will also provide a testing ground for models that try to describe the EMC effect. In addition to extending measurements of the EMC effect to lighter nuclei, ^{3}He and ^{4}He measurements can be compared directly to microscopic calculations of nuclear structure which do not exist for heavier nuclei.

2 MOTIVATION

2.1 The EMC Effect

Extensive structure function measurements have been made on nuclear targets. The European Muon Collaboration used muon scattering to measure nuclear structure functions [1]. The initial goal of using nuclear targets was to increase luminosity by increasing the target thickness, but the structure functions measured in scattering from iron and deuterium differed substantially. When they compared the cross section per nucleon, they saw an enhancement in iron below $x \approx 0.3$ and a suppression at larger values of x. Figure 1 shows the ratio σ_{Fe}/σ_D as a function of x for measurements by the EMC collaboration [1], the BCDMS collaboration [2], and SLAC experiment E139 [3]. This nuclear dependence, termed the EMC effect, has since been measured for several targets and mapped out over a large kinematical range. Following these measurements, several models have tried to explain the effect. While it is now possible to identify some of the

necessary ingredients in an explanation of the nuclear dependence of the structure function, there are still competing models that lead to significantly different pictures of the effect. An overview of measurements and models of the EMC effect can be found in ref. [4].

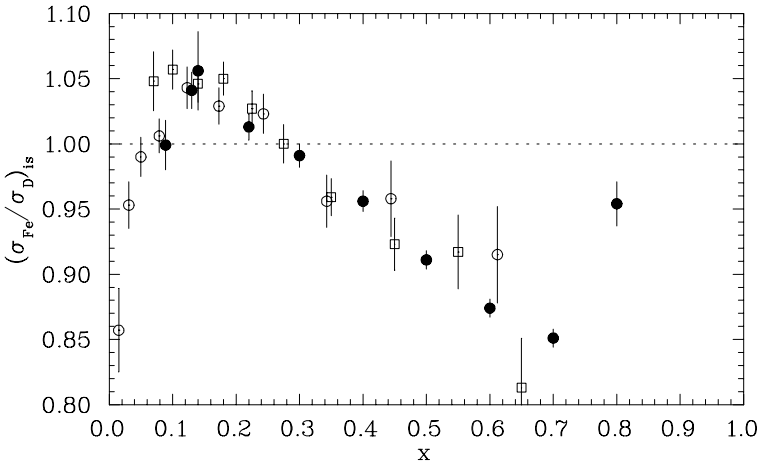

Figure 1: (σ_{Fe}/σ_D) ratios as a function of x from EMC (hollow circles), SLAC (solid circles), and BCDMS (squares). The data have been averaged over Q^2 and corrected for neutron excess (*i.e.* for isoscaler nuclei).

Several approaches have been used to try to explain the observed nuclear dependence of the cross section. If one expresses the nuclear structure function as a convolution of the proton and neutron structure functions, the modification can be generated in one of two ways. Either the nucleon structure is modified when in the nuclear medium, or the nuclear structure function is modified in the convolution due to multi-nucleon effects (binding, exchange pions, N-N correlations, etc...). Models using both types of explanation have attempted to explain the EMC effect. While many of these models have had some success, they typically reproduce only part of the observed enhancement or suppression, explain a limited x range, or are in conflict with other measurements. Calculations which simply include the momentum distribution of the nucleons predicted that the effect would be below the few percent level for $x \leq 0.6$ [5] (*i.e.* away from the quasielastic peak), which is significantly smaller than is observed. Models which also include the removal energy of the nucleon (Akulinichev *et al.*[6], Ciofi degli Atti and Luiti [7]) have been able to reproduce certain aspects of the data, but have either failed to reproduce the magnitude or the low x behavior of the effect. The nuclear dependence has also been modeled in terms of a change in the confinement radius of a nucleon bound in a nucleus. This leads to a 'swollen' nucleon, which will have a softer valence quark distribution. While this picture can reproduce the magnitude and x-dependence of the EMC effect fairly well, it requires a significant increase in the size of the nucleon ($\sim$15% for iron). This would have observable effects in other experiments, and a swelling of this size appears to be ruled out [8, 9, 10]. The EMC effect has also been modeled in terms of an enhancement of the pion field within a nucleus. The pion exchange piece of the nucleon-nucleon interaction leads to a modification of the virtual pion cloud in the nucleus, producing a shifting

of strength in x. However, this requires a pion excess that is too large to be consistent with a Drell-Yan measurement of the pion modification in nuclei [11]. Ultimately, the EMC effect may be fully described by one of the mechanisms currently being examined, by some new approach, or by some combination of these models. In order to determine which model best describes reality, we need to measure the EMC effect over as broad a range in x, Q^2, and A as possible to separate models by their specific predictions.

The most complete measurements of the EMC effect for $x \gtrsim 0.3$ come from SLAC experiment E139 [3]. They measured ratios to deuterium for ^{4}He, ^{9}Be, ^{12}C, ^{27}Al, ^{40}Ca, ^{56}Fe, ^{108}Ag, and ^{197}Au targets for a few Q^2 bins (Q^2=2 and 5 (GeV/c)^2 for $x < 0.3$; Q^2=2, 5, and 10 for $0.3 \leq x \leq 0.5$; Q^2=5 and 10 for $x > 0.5$). Figure 1 shows the E139 EMC ratio for iron as a function of x, averaged over Q^2. In addition to measuring the x-dependence, E139 examined the Q^2-dependence and A-dependence of the effect. They found no significant Q^2-dependence in the measured cross section ratios. The ratio does have a strong target dependence which, at fixed x, can be well described as a function of mass number ($\sigma_A/\sigma_D = C(x)A^{\alpha(x)}$) or as a function of ρ, the average nuclear density ($\sigma_A/\sigma_D = D(x)[1+\beta(x)\rho(A)]$). For the SLAC analysis (and in this proposal) ρ is taken to be the nuclear density (nucleons/fm^3) determined assuming a uniform sphere with a radius equal to the RMS electron scattering charge radius [3, 12]. Figure 2 shows the measured target dependence of the EMC effect, along with fits to a $\log(A)$ dependence, and a density dependence [3]. While the ^{4}He/D ratio provides the greatest sensitivity for determining if the nuclear dependence is best described as an A-dependence or a ρ-dependence, the uncertainty in the present data is large and the ratio is consistent with both parameterizations. In addition, for very light nuclei it is not clear if either of these descriptions is adequate to describe the nuclear dependence of the EMC effect. A better measurement of the A-dependence for light nuclei is necessary if we want to extend models of the EMC effect to the deuteron.

For heavy nuclei ($A \geq 9$), the magnitude of the EMC effect (the deviation from unity of σ_A/σ_D) varies with A, but the x-dependence is nearly constant. Most parameterizations of the EMC effect assume that the shape is constant or depends very weakly on A for all nuclei, except at very large values of x ($x > 0.8$), where σ_A/σ_D is dominated by the Fermi smearing. The x-dependence in ^{4}He is consistent with the heavier nuclei, but the uncertainties in the measurement are much larger, and it is not possible to rule out a significant difference in shape. Recent work by Smirnov [13] has suggested that the target ratios for $A \leq 4$ will differ from the EMC effect in heavy nuclei not only in the size of the effect, but also in the shape. He predicts that both the point of maximum suppression and the point where the EMC ratio crosses unity (at very large x) will be at lower x in ^{3}He than in ^{4}He.

At Jefferson Lab, we can improve our understanding of nuclear effects in light nuclei by measuring the EMC effect in ^{3}He and ^{4}He. Table 1 shows A, ρ, and the ratio of ρ to $\log(A)$ (taken relative to ^{27}Al) for selected nuclear targets. For the carbon and the heavier targets the difference between a linear density dependence and an A^α dependence is relatively small ($\rho/\log(A)$ varies at the 10-15% level). However, ^{3}He and ^{4}He have a significantly different dependence of density on mass number. ^{4}He is the lightest nucleus for which the EMC effect has been measured, and while it can in principle distinguish a logarithmic (A) dependence from a linear density dependence, the current measurement is not sufficient to distinguish between the two models. The proposed measurement will use a significantly denser ^{4}He target and will improve the systematic uncertainty in the ratio, which was dominated by the uncertainty in the target thickness for E139. In

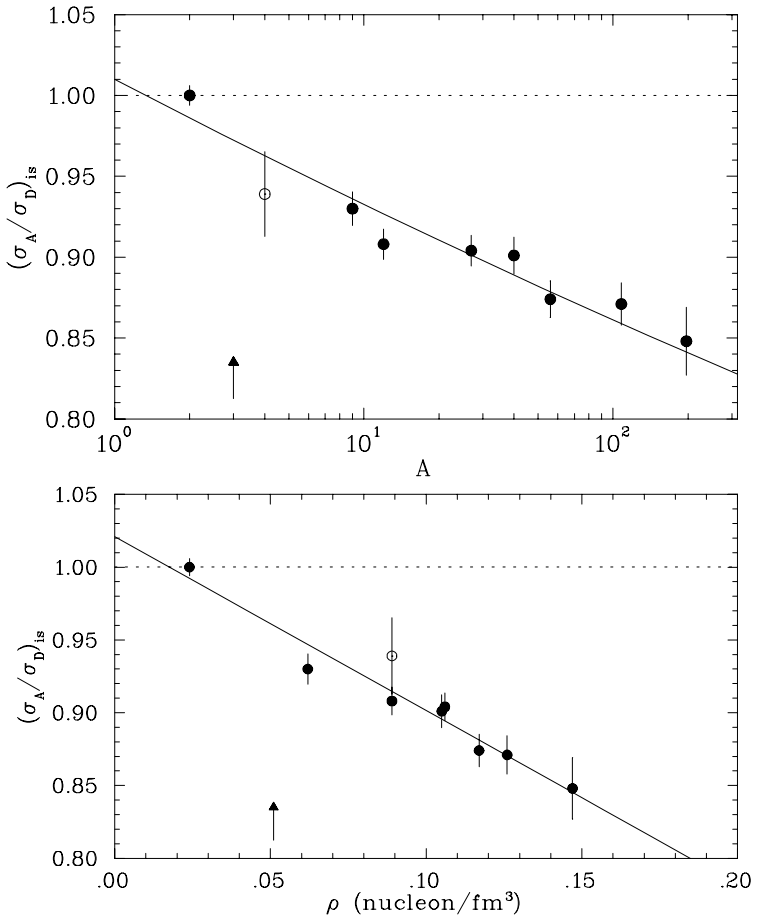

Figure 2: (σ_A/σ_D) ratios at x=0.6 from E139 plotted as a function of mass number and nuclear density. The data is averaged over all Q^2 and corrected for neutron excess. Errors include statistical uncertainties, point-to-point and target-to-target systematic uncertainties. The hollow point is ^{4}He, and the arrow indicates the location of ^{3}He.

Nucleus	A	$\rho(\mathrm{fm}^{-3})$	$[\rho/\log(A)]/[\rho/\log(A)]_{Al}$
^{2}H	2	0.024	1.08
^{3}He	3	0.051	1.44
^{4}He	4	0.089	2.00
^{9}Be	9	0.062	0.88
^{12}C	12	0.089	1.11
^{27}Al	27	0.106	1.00
^{40}Ca	40	0.105	0.87
^{56}Fe	56	0.117	0.90
^{108}Ag	108	0.126	0.84
^{197}Au	197	0.147	0.87

Table 1: Mass number and nuclear density for ^{3}He and the nuclei used in E139. The density is determined assuming a uniform sphere with a radius equal to the RMS charge radius determined from electron scattering. For ^{3}He, the proton radius is significantly different than the neutron radius. Using a calculated value for the neutron radius, or assuming that the ^{3}He neutron radius is equal to the ^{3}H proton radius, the value extracted for the nuclear density becomes somewhat higher (0.053-0.055)

addition, we will improve the statistical precision of the measurement. We expect to reduce the total uncertainty in $\sigma_{^4He}/\sigma_D$ by nearly a factor of two. ^{3}He is lower in both mass number and nuclear density than any nucleus for which the EMC effect has been measured, so the addition of data on ^{3}He will be important in parameterizing the nuclear dependence of the EMC effect in light nuclei.

We propose to measure the EMC ratio (σ_A/σ_D) for ^{3}He and ^{4}He, covering $x \gtrsim 0.3$. We will improve the uncertainty for ^{4}He, which will significantly improve our ability to distinguish and A-dependence from a ρ-dependence for the EMC effect. We will also make the first measurement of the EMC effect for $A = 3$ and large x, which will increase our range in A (and in ρ) compared to the previous measurements. The HERMES collaboration has measured σ_A/σ_D [14] for ^{3}He, but the bulk of the data is at extremely small x values (in the shadowing region). They have measurements at larger x values, but the uncertainties are large for $x > 0.5$, and while the shape is consistent with the EMC effect observed in other nuclei, the ratio is not inconsistent with unity (no nuclear effects). In addition to improving the measurements of the EMC effect in light nuclei, the proposed measurement will extend the kinematics to somewhat lower Q^2 than the previous measurements. While the SLAC measurements showed no indication of a Q^2 dependence, most of the measurements are above $Q^2 \approx 5$ (GeV/c)^2. Most of the data at lower Q^2 is for $x < 0.5$, where the deviation of the EMC ratio from unity is very small and therefore only a large relative change in this deviation would be observable in the data. The proposed measurement will allow us to investigate the Q^2 dependence down to $Q^2 \sim 1 - 2$ (GeV/c)^2.

2.2 Neutron Structure Function

Measurements of nuclear structure functions are also important for the understanding of the structure of the neutron. As free neutron targets are not available and neutron beams are too low in energy or intensity, information on the neutron structure is generally taken from measurements on nuclear targets. Current data for the neutron structure function come from measurements on deuterium and hydrogen, using models of the nuclear effects to remove the proton contribution to the deuterium measurements [15, 16]. The ability to extract the neutron structure from measurements on deuterium depends on our knowledge of the proton structure function, the deuteron momentum distribution, and the procedure used to extract the neutron component. The extraction must include a model of nuclear effects beyond the nucleon momentum distribution, and this model must be tested in order to be confident that it adequately describes all of the necessary nuclear effects.

Measurements of the neutron structure function are important for understanding the quark structure of nucleons. The difference between the structure of the neutron and the proton is sensitive to the u-quark and d-quark distributions in the proton. In particular, the ratio of the neutron to proton structure function as x approaches unity is sensitive to the high-x u-quark and d-quark valence distributions. Several predictions exist for this ratio at $x = 1$. SU(6) spin-flavor symmetry predicts $u_v^p(x) = 2d_v^p(x)$, and $d_v^n(x) = 2u_v^n(x)$, where $u_v(d_v)$ is the up(down) valence distribution in the proton or neutron. This leads to a value of $F_2^n(x)/F_2^p(x) = 2/3$ for large values of x (where the valence quarks dominate). DIS measurements indicate that SU(6) symmetry is broken, and that the proton d-quark distribution is softer than the u-quark distribution. If u-quark dominance is assumed (*i.e.* only u-quarks contribute in the limit $x \approx 1$), the prediction is $F_2^n(x)/F_2^p(x) \to 1/4$ as $x \to 1$. Other assumptions lead to a prediction that the ratio of d/u at large x is non-zero. Models by Farrar and Jackson [17], and Brodsky *et al.* [18] predict that $u/d \to 5$ as $x \to 1$, and thus $F_2^n/F_2^p \to 3/7$. The initial analysis of SLAC and EMC experiments [15, 19] indicated a value close to $1/4$, but the extraction of the neutron structure function only included corrections for the momentum distribution in the deuteron and did not include binding effects. A later reanalysis [20], including binding effects, found a value closer to the $3/7$ prediction. Figure 3 shows the extracted F_2^n/F_2^p ratio using both an on-shell prescription that only includes the momentum distribution and an off-shell prescription that includes binding. Clearly the off-shell effects are very important, and additional data that can be used to check these models is needed to determine how accurately we can extract the neutron structure from measurements on the deuteron.

We propose to measure structure functions for hydrogen, deuterium, ^{3}He, and ^{4}He for $x > 0.3$ and $Q^2 \geq 1.0$ (GeV/c)^2. The maximum Q^2 value measured will vary between $Q^2 \approx 3$ (GeV/c)^2 for the lowest value of x, to $Q^2 \approx 8$ (GeV/c)^2 for $x \sim 1$. The proposed measurement will extend the kinematic coverage to larger values of x then previous measurements. While the extraction of the neutron structure function at large values of x will still be limited by the uncertainties in modeling the nuclear effects, this data will allow us to refine these models. The EMC ratios for ^{3}He and ^{4}He will improve our ability to determine the nuclear effects in deuterium. These measurements of the EMC effect in light nuclei will help determine the appropriate way to model nuclear effects for deuterium.

In addition to looking at the nuclear dependence of the EMC effect for light nuclei, we can

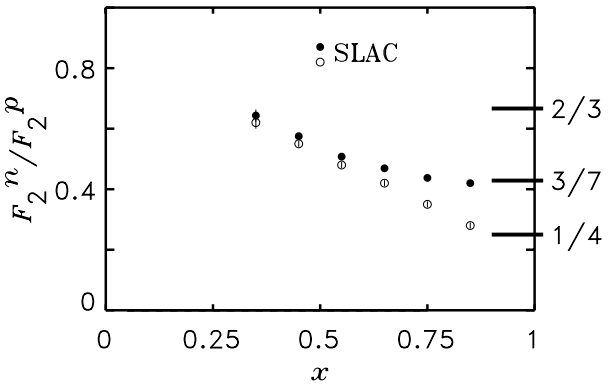

Figure 3: Ratio of F_2^n/F_2^p extracted from the SLAC measurements [3, 21] using an on-shell prescription (hollow circles) and an off-shell prescription (filled circles) to extract the neutron structure function [20].

also use these data to directly test the extraction of nucleon structure from measurements on nuclei. We can use the ^{3}He and ^{2}H measurements to extract the proton structure function to test the model of the nuclear effects used in the extraction of the nucleon structure. This procedure depends on modeling the nuclear effects in both deuterium and ^{3}He. Similarly, one can compare the neutron structure extracted from ^{2}H and ^{1}H to the structure function extracted by comparing ^{3}He and ^{1}H, or ^{4}He and ^{3}He. The nuclear effects are larger in these cases, and comparisons of the extracted neutron structure function will provide a strong test of the extraction procedure, especially for larger values of x where the nuclear effects are largest and the model dependence of the extraction is difficult to determine.

3 KINEMATIC COVERAGE

We propose a measurement of inclusive electron scattering from hydrogen and light nuclei. Scattered electrons will be measured in the HMS and SOS spectrometers, which will run independently. The majority of the data will be taken in the HMS, while the SOS will be used to make measurements of electrons from background (charge symmetric) processes and to take additional data at the largest Q^2 values. All data will be taken at the highest beam energy available (6 GeV assumed for the proposed kinematics). We will take data at 5 angles, over a range of scattered electron energies covering $0.3 < x < 1.0$. Data will be taken on hydrogen, deuterium, ^{3}He, ^{4}He, and aluminum (for subtraction of the target endcap contributions). This measurement uses the standard Hall C spectrometers and detector packages, the standard hydrogen and deuterium cryotargets, and the ^{3}He and ^{4}He targets that were used in recent pion and kaon electroproduction experiments in Hall C.

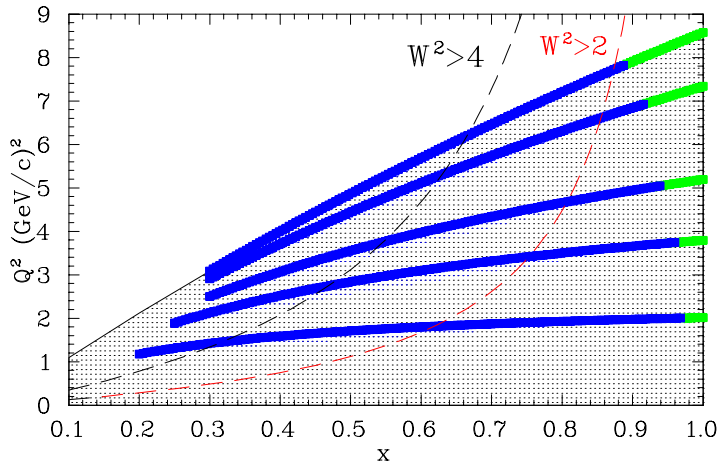

Figure 4: Overview of the proposed kinematics. The dark lines indicate the coverage for hydrogen (limited at high-x values by the rapidly falling cross section) and the grey lines indicate the additional coverage for the nuclear targets. The dashed lines correspond to W^2=2.0 and 4.0 $(\mathrm{GeV})^2$.

Figure 4 shows the proposed kinematic coverage at 6 GeV ($\theta \leq 60^\circ$) as a function of x and Q^2. The data above $Q^2 = 4.0(\mathrm{GeV/c})^2$ and at $W^2 > 4.0$ $(\mathrm{GeV})^2$ (to the left of the dashed line) are in the standardly defined DIS region. For $x < 0.65$, we will have DIS data for EMC ratios, neutron extraction, and tests of models of nuclear effects in deuterium and helium. In the DIS region, we see scaling of the structure function in x, but also in the Nachtmann variable, $\xi = 1/(1 + \sqrt{1 + 4m^2x^2/Q^2})$. ξ can be thought of as a modification to x, taking into account target mass effects. For very large Q^2, $\xi \to x$, and so in the DIS limit, the structure function will scale in ξ, and $F_2(\xi)$ will be related to the quark momentum distribution in the target, as was the case for x. However, the scaling violations at finite Q^2 will be smaller when the data is examined in terms of ξ rather than x.

While the data at higher x are below the typical cut for DIS scattering, we believe that the scaling of the structure function will continue. Inclusive measurements designed to probe $x > 1$ [22, 23] saw that scaling in scattering from nuclei occurred at kinematics far from the DIS region. Figure 5 shows the structure function for iron plotted against ξ. In iron, the smearing caused by the Fermi motion causes resonance structure and even the quasielastic peak disappear at high Q^2. Once the resonance structure has been washed out, we observe scaling at all ξ, both in the resonance region and even when the data is almost entirely dominated by quasielastic scattering. Figure 6 shows the structure function for iron as a function of Q^2 for several values of ξ. The structure function above Q^2=2-3 $(\mathrm{GeV/c})^2$ is constant to better than 10-20%. Scaling violations resulting from QCD evolution would be expected to cause variations of roughly 10% for large values of x. The largest remaining scaling violations occur at the top of the quasielastic peak (Q^2 corresponding to $x = 1$ for the fixed ξ value). Both the QCD scaling violations and the violations coming from the QE peak will be reduced at values of x somewhat lower than 1. They will also

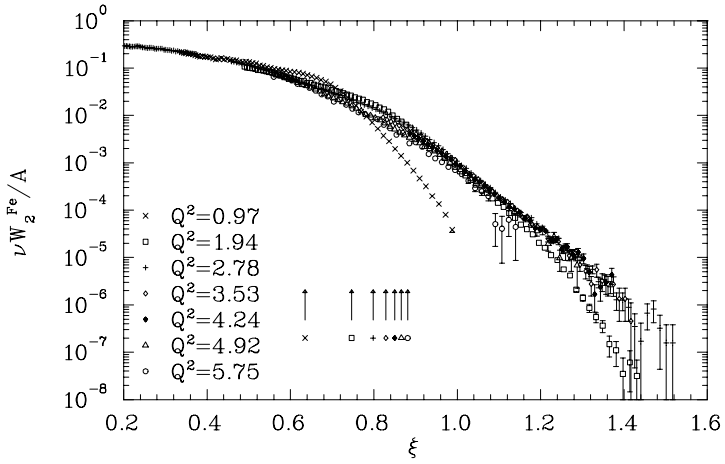

Figure 5: Structure function for Iron as a function of ξ. The data are taken at fixed scattering angle, and the quoted Q^2 is the value for $x = 1$. The arrows indicate the value of ξ corresponding to the quasielastic peak for each setting.

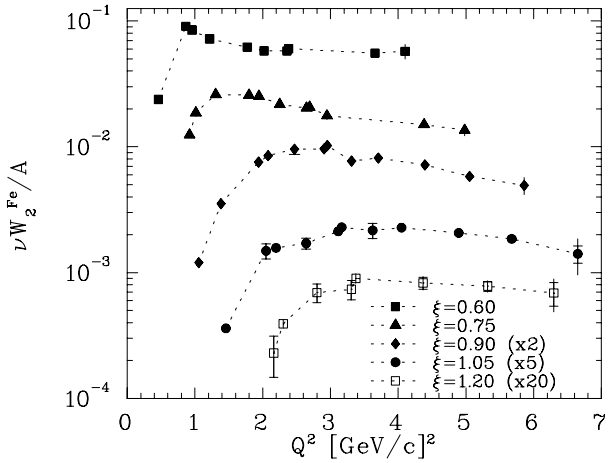

Figure 6: Structure function for Iron at fixed ξ values as a function of Q^2. Inner errors are statistical, outer errors are statistical and systematic added in quadrature.

decrease as Q^2 increases and the quasielastic contribution becomes a smaller fraction of the total cross section.

Figure 7 shows the structure function for deuterium, as a function of ξ. In this case, the quasielastic peak is clearly visible in the structure function, as is the resonance structure at lower Q^2, and the scaling that was observed in iron breaks down. As Q^2 increases the peaks move to higher ξ, but fall in strength in such a way as to roughly follow the curve in the scaling region. However, for $Q^2 \gtrsim 3$ (GeV/c)^2 the resonance structure is washed out and even the Δ resonance is no longer visible. Because deuterium has the lowest Fermi momentum, ξ-scaling should break down sooner (at higher W and Q^2) in deuterium than in any other nuclear target. The success of ξ-scaling in deuterium at extremely low values of W and relatively low momentum transfers leads us to believe that the scaling observed in the DIS region should extend to $W^2 = 2.0$ (GeV)^2 or below for the larger Q^2 values of this measurement.

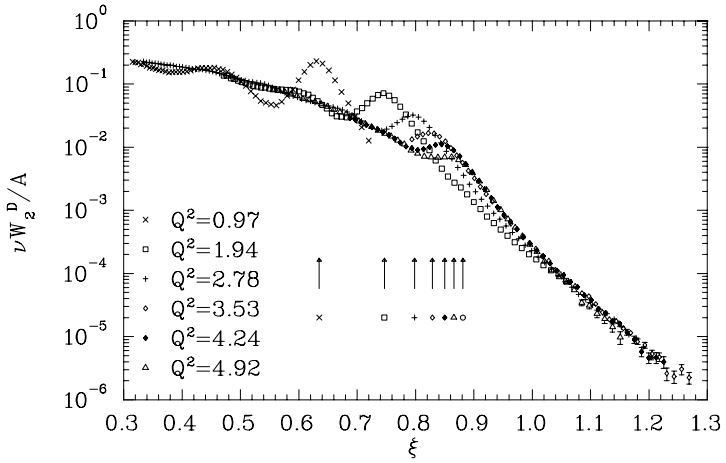

Figure 7: Structure function for Deuterium as a function of ξ. The data are taken at fixed scattering angle, and the quoted Q^2 is the value for $x = 1$. The arrows indicate the value of ξ corresponding to the quasielastic peak for each setting.

In the Bjorken limit, the parton model predicts that the structure function will scale, and that the scaling curve is directly related to the quark distributions. At finite ν and Q^2, in the 'DIS' region, scaling is observed, and it is therefore assumed that the structure function is sensitive to the quark structure of the target. It is not clear that this assumption must be correct, but the success of the scaling is taken as a strong indication that it is true. In addition, the quantitative observation of scaling is enough to make some connection between the structure function measured at finite Q^2 and in the Bjorken limit. If scaling is perfect, than the finite Q^2 structure function is equal to the high Q^2 structure function, even if one cannot explicitly show that it must be directly related to the quark distributions. While scaling is not perfect at finite Q^2, the connection to the high-Q^2 structure can be made as long as the scaling violations are well understood. Quantitative measurements of the deviation from scaling can be used to determine how precisely the data will match the value that would be measured in the scaling region. If these deviations are small, or

are largely independent of the target nucleus, then data taken at lower W^2 can also be used for measurements of nuclear effects.

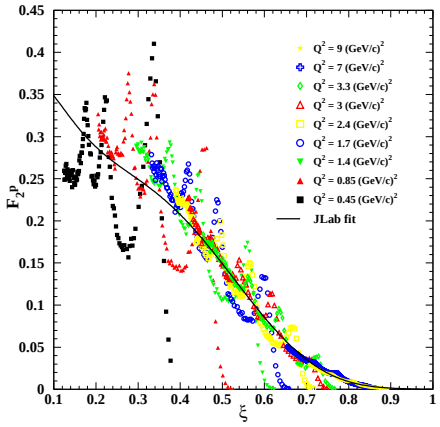

Figure 8: Hall C measurements of the resonance region structure function at low Q^2, and a fit to the combined data set.

Finally, one way to interpret the success of ξ-scaling in the resonance region is local duality. In 1970, Bloom and Gilman observed [24, 25] that the electroproduction of resonances in inclusive e-p scattering was closely related to the scaling limit in DIS scattering. Recent measurements at Jefferson Lab [26, 27, 28] have examined duality in the proton more carefully. Figure 8 shows the JLab data (plus two SLAC data sets at higher Q^2) along with a global fit to the data. For each fixed Q^2 data set, the resonance region structure function agrees with the fit globally (when averaged over the entire resonance region) and locally when averaged over any prominent resonance. This agreement extends down to $Q^2 = 1.0(\mathrm{GeV/c})^2$ without significant violations. In a nucleus, the Fermi motion of the nucleons averages over the resonances, and so rather than seeing local agreement between the DIS and resonance data, we see scaling at all values of ξ. In recent years, several people have begun to look into the theoretical basis for local duality. With a better understanding of the underlying cause of the observed duality, it may be possible to make a rigorous statement on the precision of ξ-scaling in nuclei. In the meantime, we can use the precision measurements of duality in the proton, along with our quantitative measurements of ξ-scaling in nuclei, to set an upper limit on possible scaling violations as we move from the DIS region into the resonance region. These tests will determine how far in ξ we can extend these measurements while still maintaining the quantitative connection to the quark distributions of the nucleus.

θ (deg)	E' (GeV)	x	Q^2 (GeV/c)^2	W^2 (GeV)^2	time (hours)
15	3.0-5.0 (4 settings)	0.21-1.0	1.2-2.0	0.9-5.4	22
23	2.1-4.0 (5 settings)	0.27-1.0	2.0-3.8	0.9-6.2	28
30	1.5-3.2 (6 settings)	0.29-1.0	2.4-5.2	0.9-6.9	33
45	0.75-2.1 (8 settings)	0.27-1.0	2.6-7.3	0.9-8.0	44
60	0.51-1.4 (8 settings)	0.30-1.0	3.1-8.6	0.9-8.0	79

Table 2: Kinematics for the proposed measurements. All data will be taken at 6 GeV beam energy. The run time includes time for all four targets, plus dummy running and overhead for target and momentum changes.

4 EXPERIMENTAL REQUIREMENTS

Table 2 lists the kinematics we propose to measure. Target and momentum changes are included in the total time at each scattering angle. In all cases, data will be obtained utilizing 4 cm hydrogen, deuterium, ^{3}He, and ^{4}He cryogenic targets and a 3% (radiation length) aluminum target. We will run at currents between 20 and 50 μA with 6 GeV beam energy. Table 3 is a summary of the beam time required for the measurement. In addition to the data acquisition time, we have allocated time for checkout and background measurements, spectrometer angle changes, and one changeover from hydrogen and deuterium targets to helium targets.

One of the possible significant backgrounds for the measurement is electrons coming from charge symmetric processes such as the decay of neutral pions or pair production. We will make measurements of positrons in order to subtract the charge symmetric background. JLab experiment E89-008 was run at 4 GeV over a similar range of angles. For a scattering angle of 55°, they saw a maximum e^+/e^- ratio of 15%. However, this was for $x > 1$ and a thick target. At lower x values, the e^+/e^- ratio was typically at or below 10% for the thick target. For a thin target (similar in thickness to the targets we propose to use) the e^+/e^- ratio at larger angles (74°) was $\sim$ 20%. SLAC experiment E139 ran at higher energies (8-25 GeV) and found that the charge symmetric background was negligible for most of their kinematics, and largest ($\sim$10% on deuterium) at their lowest x and Q^2 values ($x < 0.1$). We do not expect large backgrounds except possibly at the lowest electron momentum settings and largest angle. Pions are the other main source of background for the measurement. For the E89-008 experiment, the combination of lead glass shower counter and gas Čerenkov detector in the HMS (and SOS) provided pion rejection at $\sim$15,000:1 for a pion momentum of 1.0 GeV/c, and almost 100,000:1 for momenta above 1.5 GeV/c. For the high momentum settings, this is more than adequate to remove any pion

Activity	Time (hours)
Production Running	206
Target Boiling Studies	20
Angle Changes (10)	10
Target Changeover	12
e^+ measurements	8
Beam spot monitoring	4
checkout/calibration	24
Total	284 (12 days)

Table 3: Beam time request for the proposed experiment. The time shown is for HMS running. The SOS will be used for more extensive measurements of the charge symmetric background, and for parasitic data acquisition at the highest x values at 60°.

contamination from the measurement. For lower momenta, the pion contamination may become non-negligible. Since E89-008, the calorimeter has been modified so that the front two layers are read out from both ends, so we expect the pion rejection for the low momentum pions to be better than the estimates above. The only place where we anticipate the possibility of insufficient pion rejection is the lowest x values at 60°. As we will have direct measurements of the pion and charge symmetric backgrounds, we will be able to tell if the effect of these backgrounds is large. Even if they are large, these backgrounds should not have a significant impact on the proposed measurement. In both cases, the region where we anticipate possible problems is at very low x at the largest angle setting. However, the data at lower angles covers the same range in x and is only slightly lower in Q^2.

We estimate a systematic uncertainty of $\sim 3\%$ in the measured cross sections for most of the kinematics. To correct for density changes due to localized heating in the cryotargets, we will measure rate as a function of current for each target. As this effect depends on the intrinsic beam spot size in addition to the raster size, we will make regular checks of the beam size, to insure that it does not vary significantly. Many sources of uncertainty will cancel in the cross section ratios for different targets, and we estimate a final systematic uncertainty in the ratios of $\sim 1.5\%$. Table 4 shows the contributions to the systematic uncertainties in the target ratios.

5 SUMMARY

In conclusion, we request 12 days in Hall C to measure inclusive scattering from light nuclei for a broad range in x and Q^2. We will significantly improve the measurement of σ_A/σ_D in ^{4}He and make the first measurement for $A = 3$ over this x range. This will help us to understand the evolution of the EMC effect to light nuclei and allow for direct comparisons to microscopic

Source	Uncertainty	Uncertainty in σ_A/σ_D (%)
Beam Energy	$1 \cdot 10^{-3}$	0.1
HMS Angle	0.5 mr	0.1
HMS Momentum	$1 \cdot 10^{-3}$	0.1
Target Thickness	0.5-1.0%	1.2
Beam Charge	0.5%	0.7
Target Boiling	<2.0%	0.5
Endcap Subtraction	<2.0%	0.5
Acceptance	<2.0%	0.2
Radiative Corrections	<2.0%	0.2
Detector Efficiency	<1.0%	0.1
Deadtime Corrections	<1.0%	0.1
Total systematic uncertainty		1.6%

Table 4: Systematic uncertainties in the ratio σ_A/σ_D. The last column includes only the portion of the systematic uncertainty that does not cancel when taking the target ratios. Note that the uncertainty in the thickness of the deuterium target is a common uncertainty for the σ_A/σ_D ratios for ^{3}He, ^{4}He, and aluminum.

calculations of nuclear structure for few body nuclei. In addition, we will extend measurements of the the EMC effect to lower Q^2 than previous data. We will extract the neutron structure function using measurements from H, ^{2}H, ^{3}He, and ^{4}He, and make several tests of the systematic uncertainties arising from extraction of the free nucleon structure function from measurements on light nuclei. For $x \leq 0.65$, the data is in the DIS region, where the nuclear structure function is assumed to be directly sensitive to modifications of the quark distributions in the nuclei. For $x > 0.65$, we expect that ξ-scaling will still be valid for most of the Q^2 range, and we can make a quantitative measurement of scaling deviations. To the extent that these are small or target independent, we can directly use the data to study the A-dependence of the nuclear effects at these larger x values.

References

[1] J.J. Aubert *et al.*, Phys. Lett. **123B**, 275 (1983)

[2] Benvenuti *et al.*, Phys. Lett. B **189** 483 (1987)

[3] J. Gomez *et al.*, Phys. Rev. D **49** 4348 (1994)

[4] D. F. Geesaman, K. Saito and A.W. Thomas, Annu. Rev. Nucl. Part. Sci. **45** 337 (1995)

[5] A. Bodek and J.L. Ritchie, Phys. Rev. D **23**, 1070 (1981); **24**, 1400 (1981)

[6] S.V. Akulinichev *et al.*, Phys. Lett. B **158**, 485 (1985); Phys. Rev. Lett. **55**, 2239 (1985)

[7] C. Ciofi degli Atti and S. Luiti, Phys. Lett. B **225** 215 (1989); Phys. Rev. C **41**, 1100 (1990)

[8] L.L. Frankfurt and M.I. Strikman, Phys. Rep. **160**, 235 (1988)

[9] J.P. Chen *et al.*, Phys. Rev. Lett. **66**, 1283 (1991)

[10] J. Arrington *et al.*, in preparation.

[11] D.M. Alde *et al.*, Phys. Rev. Lett. **64** 2479 (1990)

[12] C.W. DeJager, H. De Vries and C. De Vries, At. Data Nucl. Data Tables **14**, 479 (1974)

[13] G.I. Smirnov, Eur. Phys. J. C **10**, 239 (1999); V.V. Burov, A.V. Molochkov, and G.I. Smirnov, Preprint arXiv:nucl-th/9904050, Apr. 1999.

[14] K. Ackerstaff *et al.*, Phys. Lett. B **475**, 386 (2000)

[15] J.J. Aubert *et al.*, Nucl. Phys. B **293**, 740 (1987)

[16] Allasia *et al.*, Zeit. Phys. C **28**, 321 (1991)

[17] G.R. Farrar and D.R. Jasckson, Phys. Rev. Lett. **35**, 1416 (1975)

[18] S.J. Brodsky, M. Burkardt and I. Schmidt, Nucl. Phys. B **441** 197 (1995)

[19] A. Bodek *et al.*, Phys. Rev. D **20**, 1471 (1979)

[20] W. Melnitchouk and A.W. Thomas, Phys. Lett. B **377**, 11 (1996)

[21] L.W. Whitlow *et al.*, Phys. Lett. B **282** 475 (1992)

[22] B. W. Filippone *et al.*, Phys. Rev. C **45**, 1582 (1992)

[23] J. Arrington, Ph.D. Thesis, Caltech (1998); J. Arrington *et al.*, to be submitted (2000)

[24] E.D. Bloom and F.J. Gilman, Phys. Rev. D **4**, 2901 (1970)

[25] E.D. Bloom and F.J. Gilman, Phys. Rev. Lett. **25**, 1140 (1970)

[26] I. Niculescu, Ph.D. Thesis, Hampton University (1999)

[27] I. Niculescu *et al.*, to be published, Phys. Rev. Lett. (2000)

[28] R. Ent *et al.*, to be published, Phys. Rev. D (2000)